

Modulation doping in $\text{Ge}_x\text{Si}_{1-x}/\text{Si}$ strained layer heterostructures: Effects of alloy layer thickness, doping setback, and cladding layer dopant concentration

R. People, J. C. Bean, and D. V. Lang
AT&T Bell Laboratories, Murray Hill, New Jersey 07974

(Received 22 October 1984; accepted 27 November 1984)

Selectively doped $\text{Ge}_x\text{Si}_{1-x}/\text{Si}$ strained layer heterostructures have been grown in a single quantum well configuration on $\langle 001 \rangle$ -Si substrate using molecular beam epitaxy. The modulation doping effect has been observed in p -type structures only; although both n - and p -type double heterostructures were grown. We have investigated the effects of: (i) alloy layer thickness (well width), (ii) doping setback, and (iii) cladding layer dopant concentration, on the hole mobilities. At present, optimum structures show peak hole mobilities in excess of $3300 \text{ cm}^2\text{V}^{-1}\text{s}^{-1}$ at 4.2 K, sheet charge densities of $3.0\text{--}14 \times 10^{11} \text{ cm}^{-2}$, and hole effective mass $m_h^* = 0.32 \pm 0.03 m_0$. It is found that the low temperature ($T \sim 10 \text{ K}$) hole mobility, in structure having $x = 0.2$ is relatively insensitive to alloy layer (well) thickness in the range $100 \text{ \AA} \lesssim L_w \lesssim L_c$; where L_c is the critical thickness marking the transition from strained layer to relaxed, misfit accommodated, alloy growth. For $L_w > L_c$, misfit dislocation scattering dramatically decreases μ_h at $T \lesssim 100 \text{ K}$; whereas for $L_w \lesssim 100 \text{ \AA}$ the hole mobility is uniformly lowered over the entire range of measurement temperatures. Doping setback and cladding layer dopant concentration affect the mobility via changes in sheet charge density, in a manner consistent with theoretical expectations. The absence of the modulation doping effect in n -type heterostructure is taken as an indication that $\Delta E_v \gg \Delta E_c$.

Heteroepitaxy of $\text{Ge}_x\text{Si}_{1-x}/\text{Si}$ offers exciting possibilities for integrated optoelectronic devices and novel FET structures. The fabrication of high mobility surface channel devices on Si substrates without the high temperature processing inherent in the synthesis of high quality SiO_2 , is especially appealing. In addition to such potential device applications, this system offers a unique opportunity for the investigation of the effects of misfit strain on the transport properties of selectively doped, indirect gap semiconductor heterointerfaces and strained layer superlattices,¹ since the lattice mismatch between Ge and Si is $\approx 4\%$.

Commensurate growth of $\text{Ge}_x\text{Si}_{1-x}/\text{Si}$ depends on the thickness of the lattice mismatched epilayers. For alloy epilayer thicknesses greater than L_c (a critical thickness which depends on Ge content x) growth is incommensurate²: the misfit strain areal energy density being high enough to nucleate dislocations. High resolution TEM,³ Rutherford back-scattering,³ and resonant Raman scattering⁴ studies have shown that thin commensurate layers of $\text{Ge}_x\text{Si}_{1-x}$ on Si experience a tetragonal strain field caused by the contraction of the alloy's in-plane lattice constant to match that of Si (i.e., the Si lattice remains rigidly in place). The (010), in-plane, compressive stress experienced by the random alloy can readily exceed $30\,000 \text{ kg F/cm}^2$, for $x \gtrsim 0.2$. This large (010) compressive stress is expected to lift the degeneracy of the $J = 3/2$ valence band edge at the Γ point, in a manner similar to that previously observed in uniaxially stressed Si.⁵ Hence, one expects a complex splitting of the $J = 3/2$ valence band edge, leading to two minimum energy surfaces of the most general nature. These perturbed valence band levels will determine the subband structure of the potential well at the heterointerface and hence, should be reflected in low

temperature oscillatory magnetoresistance (SdH) data.

In this paper we report the first detailed investigation of the effects of: (i) alloy layer thickness, (ii) doping setbacks, and (iii) cladding layer doping concentration on the mobility of selectively doped $\text{Ge}_x\text{Si}_{1-x}/\text{Si}$ heterostructures. Mobility versus temperature $10 \text{ K} \lesssim T \lesssim 300 \text{ K}$ as well as low temperature ($T \lesssim 4.2 \text{ K}$) oscillatory magnetoresistance [Shuniko-de Haas (SdH)] data have been obtained. We have observed the modulation doping effect in p -type heterostructures only; although structures having both n and p -type dopants were grown. The observation of modulation doping has obvious importance for the implementation of FET devices but moreover sheds light on the relative band alignment between Si and $\text{Ge}_x\text{Si}_{1-x}$; since the occurrence of modulation doping requires a sufficiently large discontinuity in the band edge.

We have taken the absence of modulation doping in n -type heterostructures to be an indication that $\Delta E_v \gg \Delta E_c$ (values in the literature of the band discontinuities for $\text{Ge}_x\text{Si}_{1-x}/\text{Si}$ tend to vary over a large margin^{6,7}). This assumption, together with data of Braunstein *et al.*⁸ on the indirect gap of bulk $\text{Ge}_x\text{Si}_{1-x}$ alloys leads to a band diagram for the $\text{Ge}_{20}\text{Si}_{80}/\text{Si}$ double heterostructure as shown in Fig. 1. At $x = 0.2$ the band gap difference ΔE_g is estimated at 0.10 eV .⁸ It should be noted that this value of ΔE_g is comparable to the valence band step ΔE_v for $\text{Al}_{50}\text{Ga}_{50}\text{As}/\text{GaAs}$, for which the modulation doping effect has been observed.⁹ The band bending in Fig. 1 is obtained by requiring that the Fermi level remain constant throughout the sample. This is accomplished by the transfer of holes from ionized (boron) acceptors in the P^+-Si layers to the $\text{Ge}_{20}\text{Si}_{80}$ valence-band channel which is $\Delta E_v \approx 100 \text{ meV}$ lower in energy. This is the essence of the

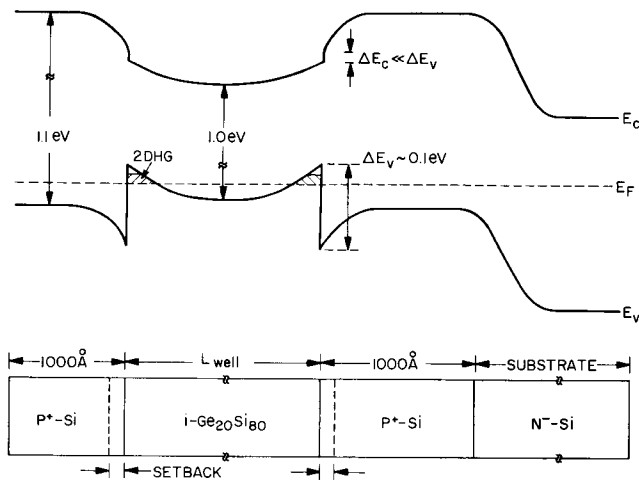


FIG. 1. Band bending diagram for $P^+-Si/i-Ge_{20}Si_{80}/P^+-Si$ strained layer double heterostructure on N^--Si substrate. We have assumed $\Delta E_c \gg \Delta E_v$ and used values for the indirect band gap of $Ge_{20}Si_{80}$ as given in Ref. 8.

modulation doping effect,¹⁰ wherein ionized acceptors are spatially separated from the conducting medium; resulting in a significant reduction in ionized impurity scattering; thus improving low temperature mobilities.

Selectively doped $Ge_{20}Si_{80}/Si$ double heterostructures were grown in a single quantum well configuration (as shown in Fig. 1) on $\langle 001 \rangle$ -Si substrates using the Si-MBE system described elsewhere.¹¹ The wide band gap Si layers were deliberately doped with either boron or phosphorus to a level $N_A - N_D \approx 10^{18} \text{ cm}^{-3}$, while the narrow gap Ge_xSi_{1-x} layer was not intentionally doped. The substrate conductivity type was always opposite to that of the doped layers. In the present study, data were obtained for samples having $x = 0.2$ and (i) $100 \text{ \AA} \leq L_w \leq 2 \text{ k\AA}$, (ii) $0 \leq L_s \leq 600 \text{ \AA}$, and (iii) $10^{17} \text{ cm}^{-3} \leq N_A - N_D \leq 10^{18} \text{ cm}^{-3}$, where L_s denotes the width of the doping setback region. p -type samples were contacted by evaporating Al and sintering at 550°C whereas n -type samples were evaporated with Au/Sb (1%) and sintered at 400°C .

The modulation doping effect was observed (to differing degrees) in all p -type samples having L_w , L_s and $N_A - N_D$ in the aforementioned range, and is demonstrated by the temperature dependent Hall data of Fig. 2 and the magnetoresistance data of Fig. 4. The two upper curves in Fig. 2 correspond to selectively doped heterostructures having $N_A - N_D = 10^{18} \text{ cm}^{-3}$, $L_w = 2 \text{ k\AA}$, and $L_s = 100 \text{ \AA}$ and $L_s = 0$; whereas the lower curve shows μ_h vs T for uniformly doped $Ge_{20}Si_{80}/Si$ epilayer of 2 k\AA thickness. The freeze-out behavior observed for $T \leq 50 \text{ K}$ in the uniformly doped epilayer is typical of 10^{18} cm^{-3} bulk Si.¹² The two upper curves in Fig. 2 exhibit: (i) peak hall mobilities which are unusually high for 10^{18} bulk Si,¹² (ii) show no strong fall-off in mobility due to ionized impurity scattering in going to low temperatures (the slight reduction in the heterostructure having no doping setback is to be expected), and (iii) the carrier densities (as shown in Fig. 3) do not show freezeout behavior saturating at a level of $6\text{--}14 \times 10^{11} \text{ cm}^{-2}$ at 4.2 K . These observations are consistent with a two-dimensional hole gas (2-DHG) at the $Si/Ge_{20}Si_{80}$ interface (or interfaces).

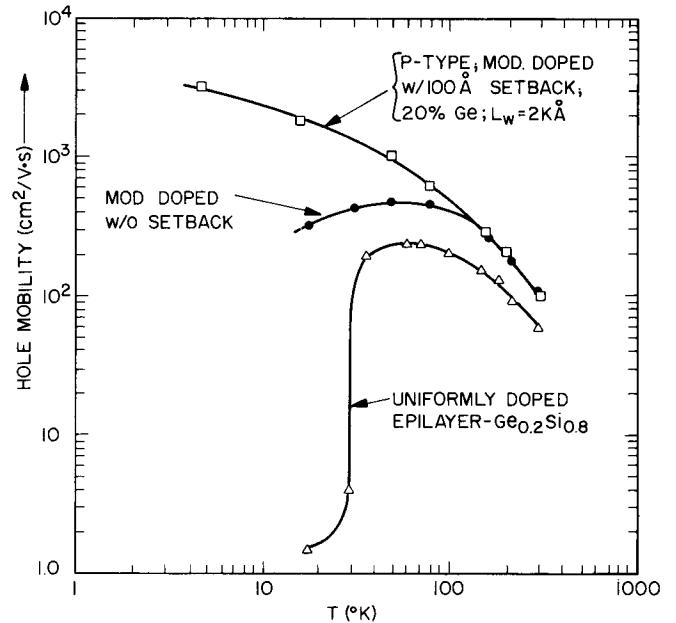


FIG. 2. Hall mobility for holes in $Ge_{20}Si_{80}/Si$ heterostructures vs temperature: (a) lower curve corresponds to uniformly doped $Ge_{20}Si_{80}$ epilayer having 2 k\AA thickness and $N_A - N_D \approx 10^{18} \text{ cm}^{-3}$, (b) center curve corresponds to a modulation doped double heterostructure of the type shown schematically in Fig. 1, but without a doping setback, (c) upper curve corresponds to same structure as center curve, except with 100 \AA doping setback.

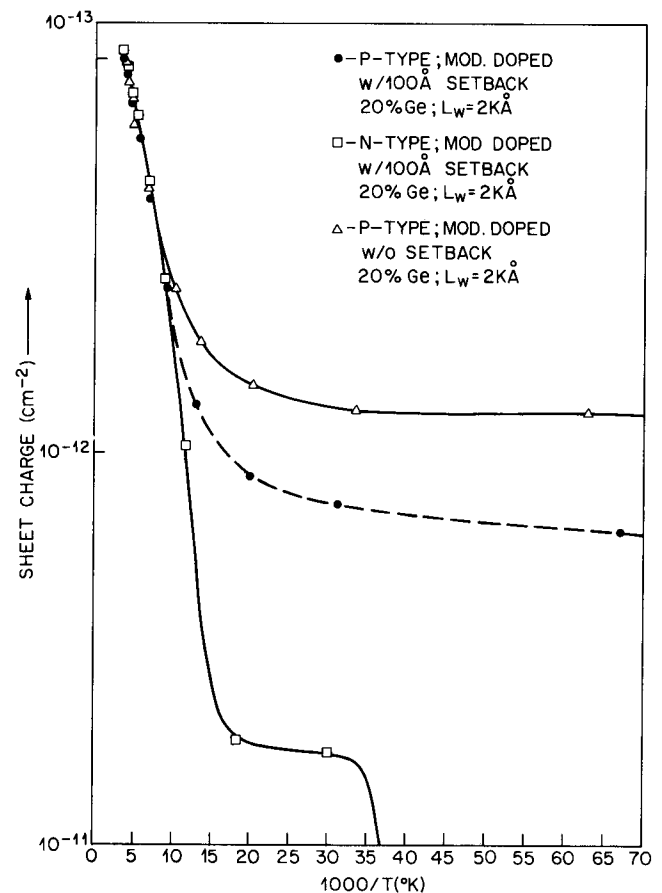


FIG. 3. Sheet charge density (cm^{-2}) vs $1000/T$ (K): (a) upper curve is for p -type modulation doped double heterostructure having $x = 0.2$, $L_w = 2 \text{ k\AA}$; $L_s = 0$, $N_A - N_D \approx 10^{18} \text{ cm}^{-3}$, (b) middle curve is identical to (a) but with 100 \AA doping setback, (c) lower curve for n -type selectively doped double heterostructure having $x = 0.2$, $L_w = 2 \text{ k\AA}$; $L_s = 0$, $N_D - N_A \approx 10^{18} \text{ cm}^{-3}$ (note freezeout behavior below $T \leq 30 \text{ K}$).

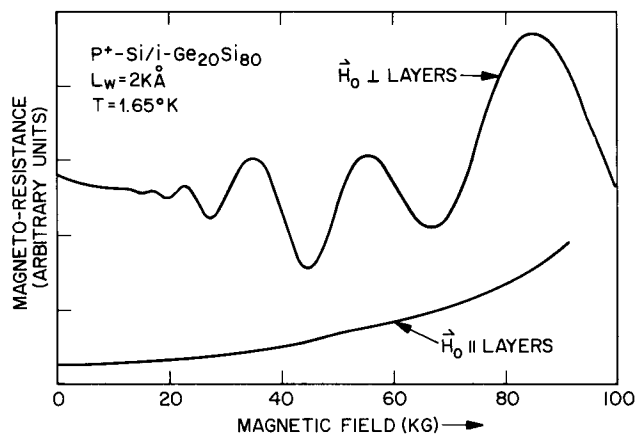


FIG. 4. Shubnikov-de Haas (SdH) data at $T \sim 1.65$ K for upper curve in Fig. 2. The strong angular dependence of the SdH peak positions confirms the two-dimensional nature of the hole gas at the $\text{Ge}_{20}\text{Si}_{80}/\text{Si}$ interface (interfaces).

From the 4.2 K value of the Hall coefficient we derive a total carrier surface density of $n_H = (6.20 + 0.10) \times 10^{11} \text{ cm}^{-2}$ and Hall mobility of $\sim 3300 \text{ cm}^2 \text{ V}^{-1} \text{ s}^{-1}$ for the upper curve ($L_s = 100 \text{ \AA}$) in Fig. 2.

Further confirmation of the two dimensionality of the hole system in the sample having $L_s = 100 \text{ \AA}$ was obtained via oscillatory magnetoresistance (SdH) measurements.^{10,14} Figure 4 shows the strong dependence of the SdH peak positions on the angle between the normal to the epilayers and the magnetic field H_0 . From the temperature dependence of the amplitude of the SdH envelope function (at $B = 45 \text{ kG}$) we derive a hole effective mass $m_h = (0.32 \pm 0.03) m_0$.

In contrast to the enhanced mobilities and absence of freezeout observed in *p*-type samples, the *n*-type selectively doped samples showed no low temperature enhancement of mobilities for $T \lesssim 80 \text{ K}$ (as shown in Fig. 5). Further, freezeout behavior was observed in the carrier surface density data, as shown in the lower curve of Fig. 3. We take these observations as an indication of a negligibly small conduction-band discontinuity (in comparison to ΔE_v).

In Fig. 6 we show the effect of alloy well width (L_w) on the temperature dependent hole mobility for three samples; each having $x = 0.2$, $N_A - N_D \approx 10^{18} \text{ cm}^{-3}$, and $L_s = 100 \text{ \AA}$ but with $L_w = 2 \text{ k\AA}$, 500 \AA , and 100 \AA , respectively. It should be noted that all three samples satisfy the criteria ($L_w < L_c \sim 2.5 \text{ k\AA}$ at $x = 0.2$) for commensurate heteroepitaxy. Low temperature mobilities ($T \lesssim 60 \text{ K}$) are almost identical for the $L_w = 2 \text{ k\AA}$ and 500 \AA samples but is uniformly lowered for the $L_w = 100 \text{ \AA}$. We suspect the $L_w = 100 \text{ \AA}$ data merely reflect the onset of enhanced scattering due to the close proximity of a second ("reverse") interface of lower quality. A similar situation has been encountered for electrons in MBE-grown GaAs/ $\text{Al}_x\text{Ga}_{1-x}\text{As}$ single heterointerfaces (cf. "reverse interface" problem¹⁵) and multiquantum wells (superlattices).¹⁶ Efforts are continuing at present (in the $\text{Ge}_x\text{Si}_{1-x}/\text{Si}$ system) to isolate the "better" interface in these heterostructures.

The effect of doping setback (L_s) on the hole mobility at $T \sim 20 \text{ K}$ is shown in Fig. 7. In these data, a series of samples were grown having fixed $N_A - N_D = 10^{18} \text{ cm}^{-3}$, $L_w = 2$

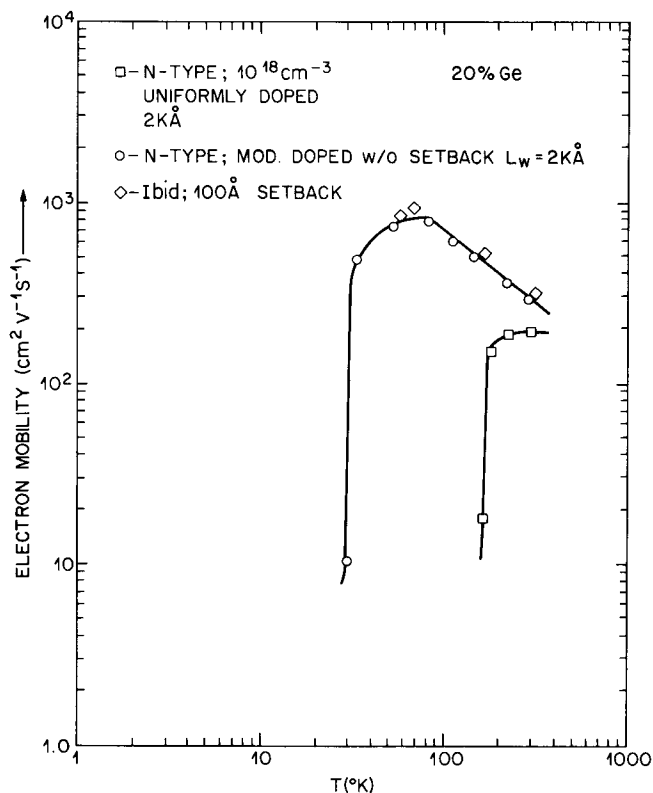


FIG. 5. Hall mobility vs temperature for electrons in: (a) a uniformly doped 2 k\AA $\text{Ge}_{20}\text{Si}_{80}$ epilayer (lower curves), (b) selectively doped *n*-type double heterostructures (upper curves)—the two types of data points correspond to samples with $L_s = 0$ and $L_s = 100 \text{ \AA}$ as shown in the inset information. Note the freezeout behavior of μ_c for $T \lesssim 30 \text{ K}$. We have assumed that this is an indication that $\Delta E_c \ll \Delta E_v$.

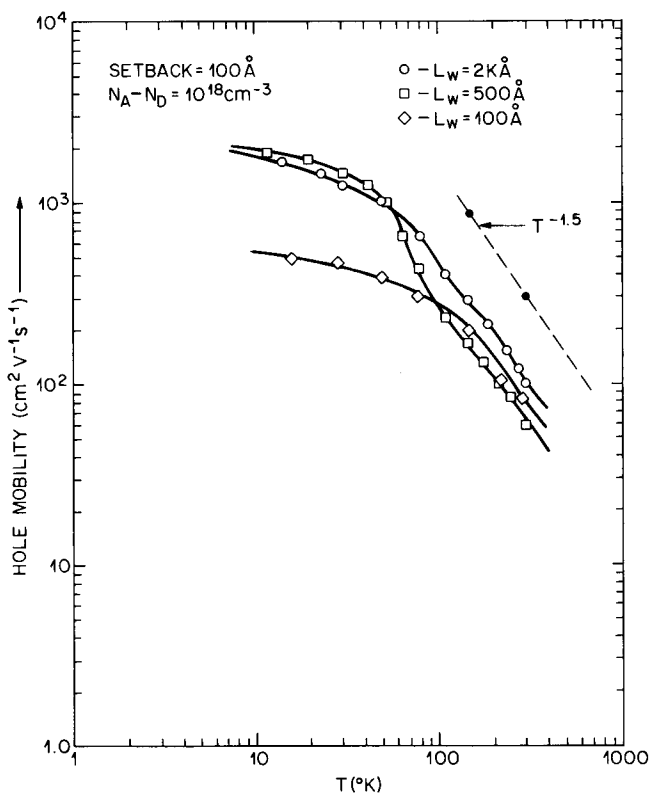


FIG. 6. Effect of alloy layer (well) thickness L_w on hole mobility for modulation doped structures with fixed $L_s = 100 \text{ \AA}$, $N_A - N_D = 10^{18} \text{ cm}^{-3}$, $x = 0.2$, and varied $L_w = 100 \text{ \AA}$, 500 \AA , and 2 k\AA .

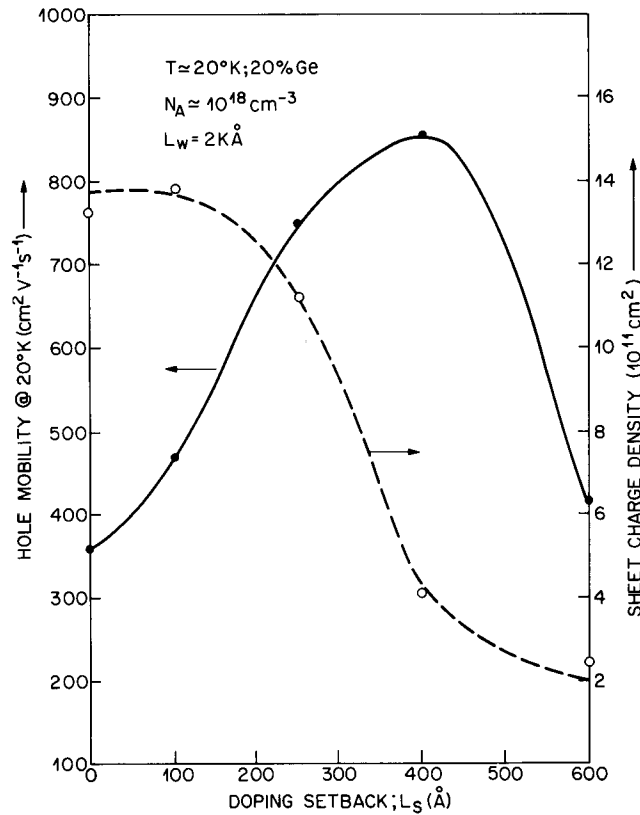


FIG. 7. Effect of doping setback L_s on hole mobility and sheet charge density in p -type selectively doped heterostructures having fixed: $L_w = 2 \text{ k}\text{\AA}$, $N_a - N_D \approx 10^{18} \text{ cm}^{-3}$, $x = 0.2$ and varied $L_s = 0; 100, 250, 400,$ and 600 \AA .

$\text{k}\text{\AA}$, $x = 0.2$, while L_s was varied between 0 and 600 \AA . It is observed that increasing setback enhances the low temperature hole mobility for $L_s \leq 400 \text{ \AA}$ at which point a further increase in L_s degrades the mobility. In this figure we also show the dependence of sheet charge density n_s on L_s . Note that n_s decreases monotonically with increasing L_s . This behavior is to be expected, since based on a simple model in which band bending in the alloy is assumed negligible (in comparison with the depletion layer band bending) one obtains:

$$n_s(L_s, N_A, \Delta E_v) \cong N_A \left\{ \left[L_s^2 + \left(\frac{2\epsilon \epsilon_0 \Delta E_v}{q^2 N_A} \right) \right]^{1/2} - L_s \right\}.$$

If one assumes that L_s effects the mobility via changes in sheet charge density n_s ; then occurrence of an optimum L_s can be interpreted by arguments previously put forth^{17,18} to explain similar data on GaAs/ $\text{Al}_x\text{Ga}_{1-x}\text{As}$ single heterointerfaces. The occurrence of an optimum L_s was interpreted as resulting from a combination of two mobility determining mechanisms: increasing L_s from $L_s = 0$ improves μ_h due to a decrease in ionized impurity scattering. Simultaneously the sheet charge density (see Fig. 7) and thereby the average hole momentum decreases leading to an increasing effectiveness of the existing scattering centers (since a Coulomb potential scatters predominantly with small wave vector). The second mechanism reduces the mobility at large L_s values leading to an overall dependence of μ_h on L_s which is roughly triangular in shape; as we have observed (Fig. 7).

Finally, the observed dependence of the low temperature

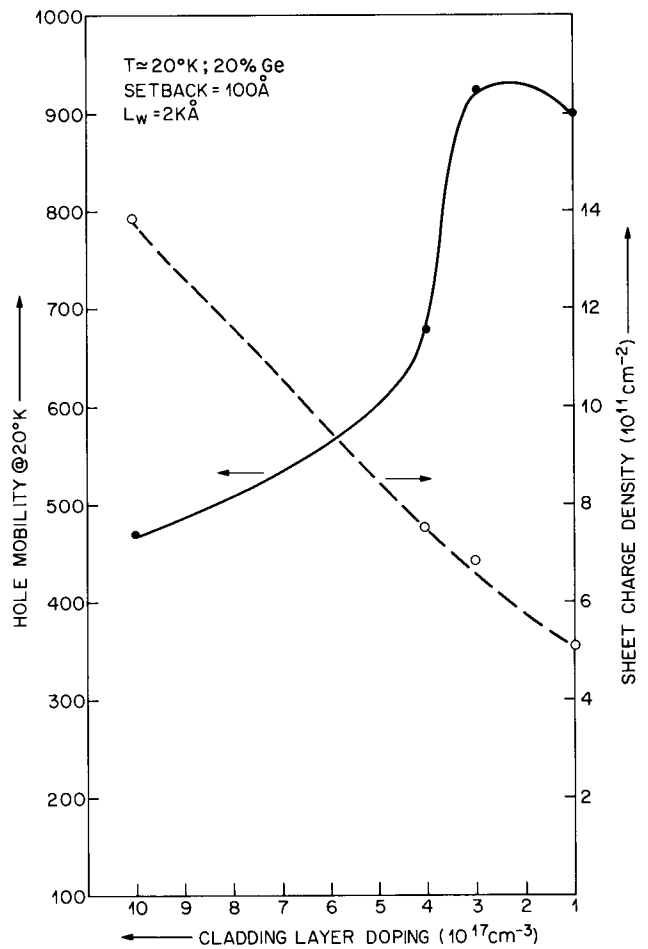


FIG. 8. Effect of cladding layer doping $N_A - N_D$ on hole mobility and sheet charge density in p -type modulation doped heterostructures having fixed: $L_w = 2 \text{ k}\text{\AA}$, $L_s = 100 \text{ \AA}$, $x = 0.2$ and varied $N_A - N_D = 1, 3, 4$ and $10 \times 10^{17} \text{ cm}^{-3}$.

hole mobility and sheet charge density on cladding layer doping concentration for a series of heterostructures having fixed $L_s = 100 \text{ \AA}$, $L_w = 2 \text{ k}\text{\AA}$, $x = 0.2$ but with $N_A - N_D$ varied from $1 \times 10^{17} \text{ cm}^{-3}$ to $1 \times 10^{18} \text{ cm}^{-3}$ in a 1, 3, 4, 10 sequence, is shown in Fig. 8. Here the mobility tends to increase as $N_A - N_D$ is lowered due to a decrease in the number of ionized impurities. Simultaneously the sheet charge density decreases. Note, however, for $N_A - N_D \leq 3 \times 10^{17} \text{ cm}^{-3}$ the advantage gained by decreasing $N_A - N_D$ is offset by the increasing effectiveness of the Coulomb potential in scattering the increasingly small wave vector holes, resulting in a decrease in μ_h for $N_A - N_D \leq 2 \times 10^{17} \text{ cm}^{-3}$.

In summary we have investigated the effects of (i) alloy well thickness, (ii) doping setback, and (iii) cladding layer doping on the low temperature hole mobility for 2-DHG systems in $\text{Ge}_{20}\text{Si}_{80}/\text{Si}$ selectively doped double heterostructures. We have found that μ_h is relatively insensitive to L_w for thicknesses: $100 \text{ \AA} \leq L_w \leq 2 \text{ k}\text{\AA}$. For $L_w \geq 2.5 \text{ k}\text{\AA}$ we no longer obtain commensurate heteroepitaxy,² whereas for $L_w \leq 100 \text{ \AA}$ quantum size effects enter. We suspect the uniform lowering of μ_h over the range of measurement temperatures ($10 \text{ K} \leq T \leq 100 \text{ K}$) is caused by the extent of the hole wave function over both heterointerfaces and further that one of these interfaces is of lower quality. Efforts are

continuing at present to determine the validity of this hypothesis. We have also found that increasing the dopant setback and/or lowering the cladding layer doping level have similar effects on the sheet charge density (n_s decreases monotonically in both cases). Although both of these effects can cause an improvement in mobility, such improvements do not persist indefinitely. In both cases the mobility shows a peak (optimum value) and decreases beyond this value, due to an increasing effectiveness of the Coulomb scattering potential at increasingly small values of the hole wave vector k_F (i.e., increasingly small sheet charge densities).

ACKNOWLEDGMENTS

We would like to thank R. T. Lynch, A. M. Sargent, K. W. Wecht, and K. Baldin for valuable technical assistance, and V. Narayanamurti and A. Y. Cho for constant encouragement in the course of these studies. We would also like to thank H. L. Störmer for useful discussions.

¹G. C. Osbourn, *J. Appl. Phys.* **53**, 1586 (1982).

²J. C. Bean, L. C. Feldman, A. T. Fiory, S. Nakahara, and I. K. Robinson,

J. Vac. Sci. Technol. A **2**, 436 (1984).

³J. C. Bean, T. T. Sheng, L. C. Feldman, A. T. Fiory, and R. T. Lynch, *Appl. Phys. Lett.* **44**, 102 (1984).

⁴F. Ciedeira, A. Pinczuk, J. C. Bean, B. Batlogg, and B. A. Wilson, *Appl. Phys. Lett.* (submitted).

⁵J. C. Hensel and G. Feher, *Phys. Rev.* **129**, 1041 (1963).

⁶G. Margaritondo, A. D. Katnani, N. G. Stoffel, R. R. Daniels, and Te-Xiu Zhao, *Solid State Commun.* **43**, 163 (1982).

⁷T. F. Kuech, M. Maenpää, and S. S. Lau, *Appl. Phys. Lett.* **39**, 245 (1981).

⁸R. Braunstein, A. R. Moore, and F. Herman, *Phys. Rev.* **109**, 695 (1958).

⁹H. L. Störmer and W. T. Tsang, *Appl. Phys. Lett.* **36**, 685 (1980).

¹⁰H. L. Störmer, R. Dingle, A. C. Gossard, W. Wiegman, and M. Sturge, *Solid State Commun.* **29**, 705 (1979); R. Dingle, H. L. Störmer, A. C. Gossard, and W. Wiegman, *Appl. Phys. Lett.* **33**, 665 (1979).

¹¹J. C. Bean, *J. Vac. Sci. Technol. A* **1**, 540 (1983).

¹²F. J. Morin and P. J. Maita, *Phys. Rev.* **96**, 28 (1954).

¹³H. L. Störmer, *Appl. Phys. Lett.* **38**, 691 (1981).

¹⁴K. von Klitzing, G. Landwehr, and G. Dorda, *Solid State Commun.* **14**, 387 (1974).

¹⁵H. Morkoc, L. C. Witkowski, T. J. Drummond, C. M. Stanchak, A. Y. Cho, and B. G. Streetman, *Electron. Lett.* **16**, 753 (1980).

¹⁶H. L. Störmer (private communication).

¹⁷J. Drummond, W. Kopp, M. Keever, H. Morko, and A. Y. Cho, *J. Appl. Phys.* **53**, 1023 (1982).

¹⁸P. Delesculse, M. Laviro, J. Chaplart, D. Delagebeaudeuf, and N. T. Linh, *Electron. Lett.* **17**, 342 (1981).